# Tracking and balance control of ball and plate system

**Article** *in* Journal- Chinese Institute of Engineers · April 2007

DOI: 10.1080/02533839.2007.9671274

CITATIONS
13

READS
616

**3 authors**, including:

C.C. Ker
National Cheng Kung University
**10** PUBLICATIONS **28** CITATIONS
SEE PROFILE

Chin E. Lin
National Cheng Kung University
**206** PUBLICATIONS **1,941** CITATIONS
SEE PROFILE

# TRACKING AND BALANCE CONTROL OF BALL AND PLATE SYSTEM

Cheng Chang Ker*, Chin E. Lin, and Rong Tyai Wang

## ABSTRACT

An extension of the traditional ball and beam system into a ball and plate system is constructed using two magnetic suspension actuators for two degree of freedom control. System characteristics of the mathematical model with control configuration are developed. For control performance, a single-chip microprocessor, serving as control kernel with basic electronic components, is designed and implemented. According to the backstepping control design procedure, the proposed controller is fabricated and tested. Several scenarios of dynamic operation, including oscillatory stabilization and circular trajectory tracking are tested to verify the system performance and capability.

***Key Words:*** ball and plate system, backstepping control, magnetic suspension actuator, circle trajectory tracking.

## I. INTRODUCTION

The ball and beam system is a typical one-dimensional nonlinear dynamic problem. Conceptually, it can be extended into a ball and plate system. A two-dimensional nonlinear electromechanical system is designed and integrated to meet the operation requirements. Either ball and beam or ball and plate are commonly created for control system modeling, design, implementation, and verification as a training tool for science and engineering practice. From the literature, the typical devices for the ball and plate system include a rigid plate with a ball rolling freely on the plate, several linear sensors for locating ball position and detecting plate deflection angle, torque generation facilities such as stepping motor, servo motor, gearbox, belt, etc. Knuplez *et al*. (2003) used the HUMUSOFT Ball and Plate Apparatus (HUMUSOFT CE151 Ball and Plate Apparatus Users Manual) to study the problem of a ball on a plate through tracking the response on a step and a sinusoidal reference signal. They used a rapid prototyping method (HUMUSOFT Real Time Toolbox for use with MATLAB Users Manual), skipping over the simulations into real experiments directly with little change. Yubazaki *et al*. (2003) proposed a fuzzy controller using the SIRMs dynamically connected fuzzy inference model for circular tracking experiments with its maximum tracking error of less than 50 mm. Rad *et al*. (2003) presented a fuzzy controller with on-line learning capability from a standard Proportional Derivative (PD) controller on tuning parameters. Such controllers have been applied successfully to the ball and plate system. Other studies on trajectory tracking or path planning using adaptive control, artificial intelligence, neuro-fuzzy approaches, and neural networks have been done (Andreev *et al*. 2002; Tsai *et al*. 1996; Pradel and Jin, 1993; Tai, 1992).

In this paper, a simple ball and plate system is presented with a simple system configuration and adaptable control implementation. The control torque is generated by a pair of hybrid magnetic suspension actuators. All of the materials and components were obtained directly from the laboratory to build the hardware platform, such as the mechanical structure of an MS actuator, the electromagnetic coil wiring, the assembly or composition of feedback sensors and control circuits from basic components. Compared with the more conventional version that has appeared

*Corresponding author. (Tel: 886-6-2392811 ext. 217; Fax: 886-6-2391915; Email: ccker@mail.ncku.edu.tw)

C. C. Ker and R. T. Wang are with the Department of Engineering Science, National Cheng Kung University, Tainan 701, Taiwan.

C. E. Lin is with the Department of Aeronautics and Astronautics, National Cheng Kung University, Tainan 701, Taiwan.

in a number of papers, which used a combination of rotary motor, gearbox, CCD camera, personal computer and its interface cards, the proposed system comprises no such expensive and complex devices. With this setup procedure, the system cost and the time of implementation can be reduced. This platform can be used not only to verify various control methodologies, but also to serve as a good training tool for system integration of electrics, mechanics, and cybernetics in an educational environment. The magnetic suspension (MS) actuator is designed to levitate the plate from two sides, with the pivot at the central point of the plate to control the plate deflection angle ($\theta_x$ and $\theta_y$) in two degrees of freedom. The MS actuator is designed for one-dimensional position control up or down from its original operation point (Lin *et al*. 2005). A Touch Control Panel (TCP) on the aluminum plate is used as the position sensor for an 85-gram iron ball rolling freely on it, the TCP's sensing principle and resolution will be discussed in more detail at Section III.2. The hardware of the micro-processor circuit is constructed using an embedded single-chip CPU to provide position controls for the magnetic suspension actuator. Using the least-square curve-fitting method, the electromagnetic (EM) force model for the actuator, the transfer characteristic of the ball position sensor, plate deflection angle sensor and each sub-system in the control circuit are identified for system design, with detailed discussion in Section III. From Euler-Lagrange's theory, a mathematical model is derived to describe the dynamic behavior. According to the backstepping control design procedure, a suitable controller is designed and implemented onto a single-chip CPU. The force and current characteristics can be derived exactly from the manipulation steps. This leads to a successful control of the MS actuators on the proposed ball and plate system.

## II. APPARATUS DESCRIPTION

In the proposed ball and plate system, the torque is generated by two hybrid magnetic suspension (MS) actuators (Lin *et al*. 2005). The basic structure of the MS actuator contains embedded permanent magnets to interact with EM coils to exert enduring force on the motion support. The apparatus in the proposed system comprises an aluminum base to hold all components, a TCP on an aluminum plate for positioning, a pivot at the plate center as the origin, two MS actuators on two sides of motion plate, an 85-gram free-run iron ball, and an embedded single-chip CPU controller hardware. The TCP plate is divided into four quadrants supported by a 250 mm length aluminum cylinder on the pivot with two MS actuators on two sides of this plate. Two identical

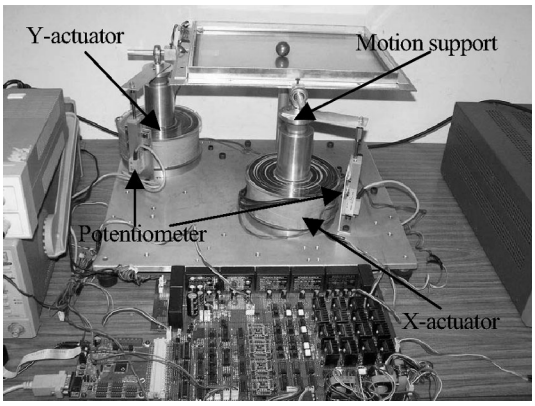


Fig. 1 Ball and plate test platform (back view)

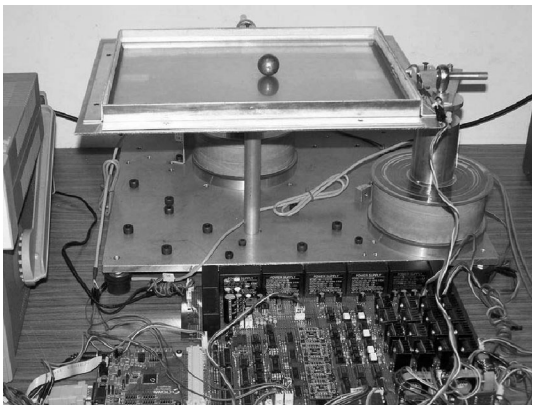

Fig. 2 Ball and plate test platform

MS actuators are introduced as motion supports for torque control. One of the MS actuators is located at 225 mm from the origin on the X-axis, named "X-actuator", while the other is located at 185 mm from the origin on the Y-axis, named "Y-actuator". The motion supports can be driven upward or downward by EM force from original operation locations to turn the plate in either pitch or roll motion from one side. Two potentiometers are applied to measure plate deflection angle from the motion supports shown as in Fig. 1. Its detailed discussion will be presented at Section III.2. A single-chip CPU with software and an electronic circuit board are built as the control kernel. The proposed ball and plate platform apparatus is shown as in Fig. 1 and Fig. 2. By controlling the X-actuator or Y-actuator, the plate will perform roll or pitch motion to activate the free-run iron ball.

## III. CONTROL SYSTEM AND STATE VARIABLE MEASUREMENT

To implement the proposed system, several subsystems and components are designed and integrated

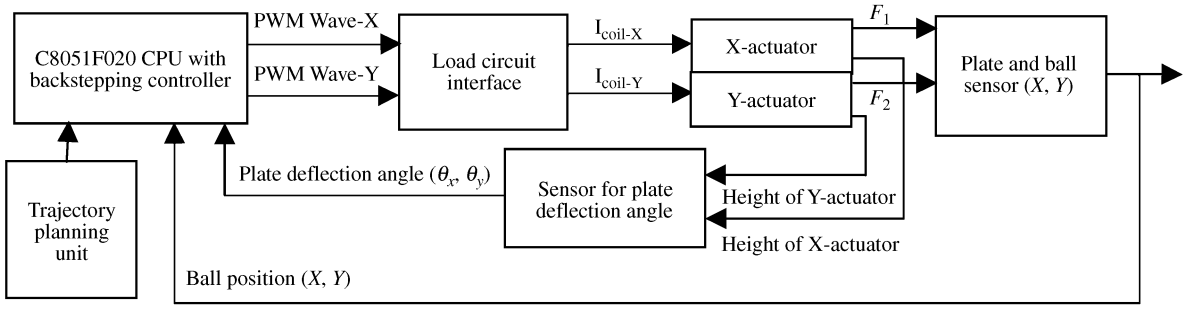


Fig. 3 Block diagram for control system

with its function block diagram as shown in Fig. 3. A single-chip micro-controller C8051F020 CPU (Cygnal Integrated Products Inc. for C8051F020 Data Sheet) is designed as the control kernel. According to the backstepping control principle, the controller is fabricated onto the single-chip CPU with C language. A trajectory planning unit is arranged to assign a reference trajectory for the next sampling cycle. With feedback of the ball position and plate deflection angle under proper control sequence, two PWM waveforms are generated with their duty cycles proportional to the controller input requirement. These waveforms are converted into load current to drive their corresponding actuators.

Two sets of H-bridge circuits consisting of four power MOSFETs are employed to convert the PWM waveform into load current according to its duty cycle to drive the EM coils of the MS actuators. There are some isolation and logic gates for each power transistor to isolate high-voltage glitches and noise. Because the driving current may drift due to temperature variation, a Hall sensor is connected in series to the EM coil for load current measurement with its output signal feeding back to the CPU to maintain the constant current. The control circuit consists of an embedded single-chip micro-processor C8051F020 CPU, A/D, D/A, and some electronic components fabricated in the laboratory. A software program in C language was completed in the development phase to promote program efficiency. With the function successfully verified, the program is revised and promoted. The C language in combination with the assembly language is coded into the execution program at the final phase. The implementation program takes 24k bytes in memory space and its CPU time is less than 10 ms. The multiple interruption technique is applied in the program to avoid task conflicts.

## 1. Identification of MS Actuator

Magnetic field distribution in space is characterized by its nonlinear property, making it difficult for all large gap MS systems to be applied with the conventional mathematical model of EM interaction force. The EM force is a function of EM coil current ($i$) to distance ($z$) in terms of $F(i, z)$. A model for the MS actuator is established by real measurement and calibration. A current to force measurement is carried out to establish the force model (Lin and Jou, 1993), (Lin *et al.* 2005). The current $i$ is defined as the EM coil current, and the gap $z$ is defined as the motion distance of the MS actuators. Both variables $i$ and $z$ are changed in small step increments to constitute the exerting force. The coil current is measured $-3.6 < i < 3.6$ A. with $\Delta i = 0.2$ A., and the gap distance is determined by $0 < z < 39$ mm with $\Delta z = 1$ mm. Assume that the force model is a second-order function of $i$ and $z$, and is written as:

$$F(i, z) = a_{11}z^2 + a_{12}zi + a_{13}i^2 + a_{14}z + a_{15}i + a_{16},$$

where $a_{ij}$ are parameters to be determined. Using the least-square curve-fitting method with parameter minimization, the parameters for the force model can be obtained. By using the software package "Original", the pattern for this model is reconstructed in three dimensions (3D) as shown in Fig. 4.

For the backstepping controller, $F(i, z)$ is converted into load current ($i$) as a dependent variable in terms of EM force ($F$) and motion support displacement ($z$) as:

$$i(F, z) = a_{21}F^2 + a_{22}Fz + a_{23}z^2 + a_{24}F + a_{25}z + a_{26}. \quad (1)$$

The coefficients of Eq. (1) are obtained from experiments as:

$$a_{21} = -0.038502634,\ a_{22} = 161.66076,$$

$$a_{23} = -704.4245,\ a_{24} = 1.5224165,$$

$$a_{25} = 86.296035,\ a_{26} = -0.64591535$$

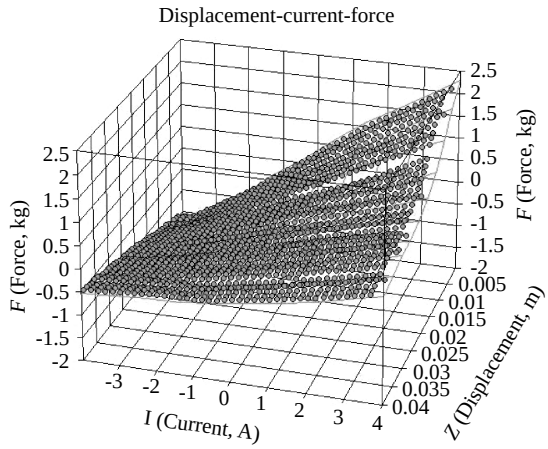


Fig. 4 The 3D characteristic of MS actuator for *F*, *i* and *z*

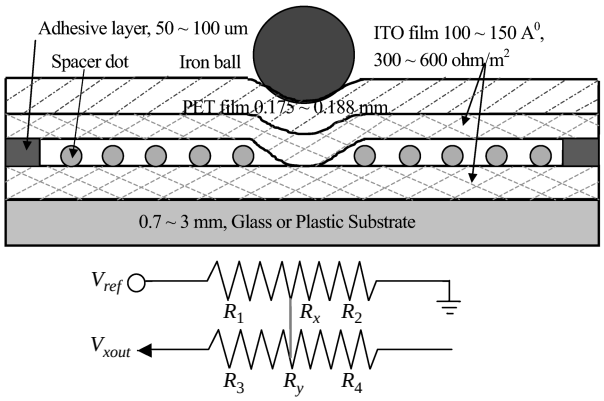


Fig. 5 Structure of TCP for ball position sensing

## 2. The State Variable Measurement

According to the TCP sensing principle for plane positioning as shown in Fig. 5, the Indium Tin Oxide (ITO) layer deposited on the glass substrate is identified as a sheet of resistance film of $R_y$; while the other layer is $R_x$. When the weight of the iron ball falls on the Polyethylene Terepthalate (PET) film, these two layer sheets of resisters will come into contact to form a potentiometer effect. By interactive bias to either terminal of $R_x$ or $R_y$, the output voltage of the contact point is obtained from the other un-biased resistance terminal. According to the TCP specifications from the supplier, (1) the sensitive area to touch force is about 693 $cm^2$ in thickness 100 Å to 150 Å; (2) the TCP resistance coefficient is around 300 to 600 ohm/$m^2$; (3) the effective to safety touch force on PET film is equivalent to around 50 ~ 100 grams. Based on these parameters, the test weight of iron ball is chosen at 85 grams. The PET film deforms where the iron ball is located, $R_x$ and $R_y$ are short circuited as a crossing line, as shown in Fig. 5, to divide $R_x$ into $R_1$ and $R_2$ as a voltage divider to output $V_{xout}$ from $V_{ref}$. To find the ball position transfer equation, let the central point on the plate be the origin, then the X-axis is ±160 mm, and the Y-axis is ±120 mm.

By the curve-fitting method, the ball position transfer functions on the plate are obtained as:

$$x = -7.789 \times 10^{-5} \times V_{xout} + 0.16421, \text{ (m)} \quad (2a)$$

$$y = 5.9488 \times 10^{-5} \times V_{yout} - 0.12516. \text{ (m)} \quad (2b)$$

where $x$ and $y$ are ball positions, $V_{xout}$ and $V_{yout}$ are voltage divider outputs, respectively on the X- and Y-axis. The transfer curve of the ball position to sensor output on the X- and Y-axis has a resolution of 0.1 mm.

For the plane deflection sensing, two 5 k Ohm, 50 mm potentiometers are arranged to sense the MS actuator at level height of the motion support as shown in Fig. 1. By applying 10 V DC reference voltage, these two sensors provide a resolution of 200 mV/mm. These two MS actuators are located at two sides of the plate, the X-actuator is used for pitch angle control along the X-axis ($\theta_x$), and the Y-actuator is for roll-angle control along the Y-axis ($\theta_y$). These two actuators are limited to 40 mm travel range, and the height of the middle point is equal to the height of the pivot, so that the each MS actuator can only be operated within 20 mm up or down from its neutral point. By this arrangement, the proposed system gets a symmetrical deflection angle range for both $\theta_x$ and $\theta_y$. Using curve-fitting, the actuator transfer equations can be expressed as:

$$H_{X\text{-}ACT} = -0.011151 \times V_{X\text{-}ACT} + 27.8774, \text{ (mm)}$$

$$H_{Y\text{-}ACT} = -0.011424 \times V_{Y\text{-}ACT} + 28.1233, \text{ (mm)}$$

for the X- and Y-actuator, where the $V_{X\text{-}ACT}$ and $V_{Y\text{-}ACT}$ are the potentiometer outputs, they are proportional to the travel distance of the corresponding actuator. $H_{X\text{-}ACT}$ and $H_{Y\text{-}ACT}$ are the level height of the motion support of MS actuators. Under this arrangement, the plate deflection angle for the X- and Y-axis can be shown as:

$$\theta_x = \arcsin\left(\frac{H_{X-ACT}}{225}\right), \text{ (rad.)} \quad (3a)$$

$$\theta_y = \arcsin\left(\frac{H_{Y-ACT}}{185}\right). \text{ (rad.)} \quad (3b)$$

After converting the actuator level height of ±20 mm into deflection mechanically, the plate deflection angle $\theta_x$ is bounded within ±0.089 radians, but $\theta_y$ is within ±0.1083 radians. By sensor measurement, four different feedback state variables are obtained as the

**Table 1 Specific system parameters**

| Symbol | Parameters | Description |
|---|---|---|
| $m_b$ | 0.085 kg | Mass of the ball |
| $R$ | 0.025 m | Radius of the ball |
| $h$ | 384 mm | The plate's length at X-axis |
| $b$ | 303 mm | The plate's width at Y-axis |
| $J_b$ | 4.3226e-6 kg-m$^2$ | The inertia of mass moment of ball |
| $J_{px}$ | 1.032e-2 kg-m$^2$ | The inertia of mass moment of plate in the X-axis |
| $J_{py}$ | 1.677e-2 kg-m$^2$ | The inertia of mass moment of plate in the Y-axis |

ball position ($x$, $y$) and the plate deflection angle ($\theta_x$, $\theta_y$). Extra state variables such as the ball velocity and plate deflection angle velocity are required for control performance. By the first-order-finite difference, the ball velocity ($\dot{x}$, $\dot{y}$) and plate deflection angle velocity ($\dot{\theta}_x$, $\dot{\theta}_y$) are expressed as:

$$\dot{x}(n) = \frac{x(n) - x(n-1)}{\Delta t}, \text{ (m/s)} \tag{4a}$$

$$\dot{\theta}_x(n) = \frac{\theta_x(n) - \theta_x(n-1)}{\Delta t}, \text{ (rad./s)} \tag{4b}$$

where $\Delta t$ is the sampling interval, and likewise for $\dot{y}(n)$ and $\dot{\theta}_y(n)$. From the above equations, the controller receives enough information to implement a control algorithm. Although the noise amplification in the first-order-finite difference operation may be a problem, in the proposed system, the noise problem can be ignored since the sampling interval ($\Delta t$) at 10 ms can update so quickly it overwhelms the noise.

## IV. SYSTEM MODELING

The proposed system is depicted in Fig. 6 with a TCP on a rectangular aluminum plate. There are two MS actuators for two sides of the plate with a pivot at the center of the plate as the supporting structure. Let MS actuator 1 act at the point $P_1(a_1, b_1)$ and contribute the magnetic force $F_1(a_1, b_1)$ for the proposed system, and likewise let MS actuator 2 act at the point $P_2(a_2, b_2)$ for $F_2(a_2, b_2)$. The difference in deflection angle between the plate and the X-axis is presented to $\theta_x$, and correspondingly, that between the plate and the Y-axis is presented to $\theta_y$. By controlling the level height difference between these two MS actuators, the plate deflection results in the iron ball rolling on the plate. Some specific parameters are listed in Table 1.

To derive the motion equations for the proposed system, assuming that the ball remains in contact with the plate only rolling, not sliding, the total kinetic energy (K.E.) of the proposed system consists of terms

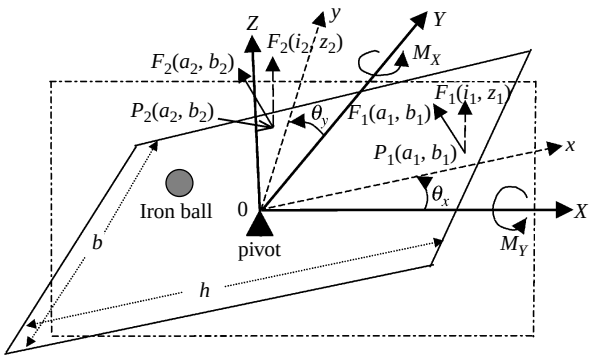


Fig. 6 The mathematical model for ball and plate system

on: (1) plate due to plate rotation, (2) ball at fixed position due to plate rotation, (3) ball in vertical direction due to plate rotation, and (4) ball relative to plate respectively. The equation can be denoted as:

$$K.E. = \frac{1}{2}[J_{px}\dot{\theta}_x^{\,2} + J_{py}\dot{\theta}_y^{\,2} + J_b(\dot{\theta}_x^{\,2} + \dot{\theta}_y^{\,2}) + m_b(x\dot{\theta}_x + y\dot{\theta}_y)^2 + (m_b + \frac{J_b}{R^2})(\dot{x}^2 + \dot{y}^2)]. \tag{5}$$

On the other hand, the potential energy, including ball, plate, and actuator forces, can be expressed as:

$$\begin{aligned} W &= -m_b g \times (x\sin\theta_x + y\sin\theta_y) + F_1(i_1, z_1) \\ &\quad \times (a_1\sin\theta_x + b_1\sin\theta_y) + F_2(i_2, z_2) \\ &\quad \times (a_2\sin\theta_x + b_2\sin\theta_y) \\ &= -m_b g \times (x\sin\theta_x + y\sin\theta_y) + F_1(a_1, b_1) \\ &\quad + F_2(a_2, b_2). \end{aligned} \tag{6}$$

where $F_1(i_1, z_1)$ and $F_2(i_2, z_2)$ are the EM forces, which will be written in short form as $F_1$ and $F_2$ in this paper, and are generated by the X-actuator and Y-actuator respectively. By applying Euler-Lagrange's equation as Eq. (5) and Eq. (6), the mathematical model for the proposed system can be given by,

$$(m_b + \frac{J_b}{R^2})\ddot{x} - m_b(x\dot{\theta}_x + y\dot{\theta}_y)\dot{\theta}_x = -m_b g \sin\theta_x ,$$

$$(m_b + \frac{J_b}{R^2})\ddot{y} - m_b(x\dot{\theta}_x + y\dot{\theta}_y)\dot{\theta}_y = -m_b g \sin\theta_y ,$$

$$(J_{px} + J_b + m_b x^2)\ddot{\theta}_x + m_b(2x\dot{\theta}_x\dot{x} + x\dot{\theta}_y\dot{y} + y\dot{\theta}_y\dot{x} + xy\ddot{\theta}_y) = (F_1 a_1 + F_2 a_2 - m_b g x)\cos\theta_x,$$

$$(J_{py} + J_b + m_b y^2)\ddot{\theta}_y + m_b(2y\dot{\theta}_y\dot{y} + y\dot{\theta}_x\dot{x} + x\dot{\theta}_x\dot{y} + xy\ddot{\theta}_x) = (F_1 b_1 + F_2 b_2 - m_b g y)\cos\theta_y.$$

In order to find out the controller conveniently, by re-defining state variables as:

$$X = (x_1, x_2, x_3, x_4, x_5, x_6, x_7, x_8)^T = (x, \dot{x}, \theta_x, \dot{\theta}_x, y, \dot{y}, \theta_y, \dot{\theta}_y)^T.$$

the proposed system can be written in state-space form as,

$$\begin{bmatrix} \dot{x}_1 \\ \dot{x}_2 \\ \dot{x}_3 \\ \dot{x}_4 \\ \dot{x}_5 \\ \dot{x}_6 \\ \dot{x}_7 \\ \dot{x}_8 \end{bmatrix} = \begin{bmatrix} x_2 \\ A(x_1 x_4^2 + x_4 x_5 x_8 - g\sin x_3) \\ x_4 \\ 0 \\ x_6 \\ A(x_5 x_8^2 + x_1 x_4 x_8 - g\sin x_7) \\ x_8 \\ 0 \end{bmatrix} + \begin{bmatrix} 0 & 0 \\ 0 & 0 \\ 0 & 0 \\ 1 & 0 \\ 0 & 0 \\ 0 & 0 \\ 0 & 0 \\ 0 & 1 \end{bmatrix} \begin{bmatrix} u_x \\ u_y \end{bmatrix},$$

where $A = \dfrac{m_b}{m_b + \dfrac{J_b}{R^2}}$, (7)

$$u_x = \frac{1}{(J_{px} + J_b + m_b x_1^2)(J_{py} + J_b + m_b x_5^2) - (m_b x_1 x_5)^2} \times \{m_b x_1 x_5[m_b(2x_5 x_6 x_8 + x_2 x_4 x_5 + x_1 x_4 x_6) + (m_b g x_5 - F_1 b_1 - F_2 b_2)\cos x_7] - (J_{py} + J_b + m_b x_5^2)[m_b(2x_1 x_2 x_4 + x_1 x_6 x_8 + x_2 x_5 x_8) + (m_b g x_1 - F_1 a_1 - F_2 a_2)\cos x_3]\}, \quad (8)$$

$$u_y = \frac{1}{(J_{px} + J_b + m_b x_1^2)(J_{py} + J_b + m_b x_5^2) - (m_b x_1 x_5)^2} \times \{m_b x_1 x_5[m_b(2x_1 x_2 x_4 + x_1 x_6 x_8 + x_2 x_5 x_8) + (m_b g x_1 - F_1 a_1 - F_2 a_2)\cos x_3] - (J_{px} + J_b + m_b x_1^2)[m_b(2x_5 x_6 x_8 + x_2 x_4 x_5 + x_1 x_4 x_6) + (m_b g x_5 - F_1 b_1 - F_2 b_2)\cos x_7]\}. \quad (9)$$

Obviously, this system is a nonlinear two-dimensional system. Although there are so many different control laws that can be used to stabilize the proposed system, this paper chooses the backstepping controller to demonstrate the controller design procedure step by step. These procedures begin from the development of motion equations, and go through deriving the equations of electromagnetic force for these two MS actuators.

## V. THE CONTROLLER DESIGN

In order to reduce the complexity of the proposed system, the velocity and acceleration of plate deflection are limited in the control algorithm. From the preliminary tests, since the coupling effect is not significant and can be neglected, the proposed system appears to be two independent ball and beam systems (Lin *et al*. 2005), and can be approximately decomposed into two independent systems for the X-axis and Y-axis as:

$$\begin{bmatrix} \dot{x}_1 \\ \dot{x}_2 \\ \dot{x}_3 \\ \dot{x}_4 \end{bmatrix} = \begin{bmatrix} x_2 \\ A(x_1 x_4^2 - g\sin x_3) \\ x_4 \\ 0 \end{bmatrix} + \begin{bmatrix} 0 \\ 0 \\ 0 \\ 1 \end{bmatrix} u_x', \quad (10a)$$

$$\begin{bmatrix} \dot{x}_5 \\ \dot{x}_6 \\ \dot{x}_7 \\ \dot{x}_8 \end{bmatrix} = \begin{bmatrix} x_6 \\ A(x_5 x_8^2 - g\sin x_7) \\ x_8 \\ 0 \end{bmatrix} + \begin{bmatrix} 0 \\ 0 \\ 0 \\ 1 \end{bmatrix} u_y'. \quad (10b)$$

Then Eqs (8) and (9) can be reduced to:

$$u_x' = \frac{1}{J_{px} + J_b + m_b x_1^2}[(F_1 a_1 + F_2 a_2 - m_b g x_1)\cos x_3 - 2m_b x_1 x_2 x_4], \quad (11a)$$

$$u_y' = \frac{1}{J_{py} + J_b + m_b x_5^2}[(F_1 b_1 + F_2 b_2 - m_b g x_5)\cos x_7 - 2m_b x_5 x_6 x_8]. \quad (11b)$$

These two independent systems have similar characteristics. The following discussion on the controller development procedure for the X-axis can also be extended for the Y-axis. The ball and plate system is nonlinear. The controller design expects not only closed-loop stability, but also tracking performance. According to Lyapunov stability theory for a low-order controller, the proposed controller is derived in four steps with a specific control law. The final step can verify system stability with controller design. The ball and plate system does not satisfy the constraints of a strict feedback system, the difference from the usual backstepping controller design is discussed (Zhao and Kanellakoulos, 1998), (Khalil, 2002), (Miroslav *et al*. 1995). Following the system model in Eqs. (10) and (11), the design steps are formulated as:

Step 1: Define the error variables $e_1 = x_1 - y_{dx}$ and $e_2 = x_2 - \alpha_1$, for $\alpha_1$ is the first stabilizing function to be determined, $y_{dx}$ is the trajectory to be tracked by the proposed control system, the time derivative of $e_1$ as: $\dot{e}_1 = \dot{x}_1 - \dot{y}_{dx} = x_2 - \dot{y}_{dx} = (e_2 + \alpha_1) - \dot{y}_{dx}$. By choosing the Lyapunov function $V_1 = \frac{1}{2}e_1^2$, to compute its time derivative:

$$\dot{V}_1 = e_1\dot{e}_1 = e_1(e_2 + \alpha_1 - \dot{y}_{dx}), \tag{12}$$

let $\alpha_1 = -c_1e_1 + \dot{y}_{dx}$, and $c_1 > 0$ then,

$$\dot{e}_1 = -c_1e_1 + e_2, \tag{13}$$

$$\dot{V}_1 = -c_1e_1^2 + e_1e_2, \ \dot{V}_1 \text{ is indefinite.}$$

Step 2: According to the computation result of step 1, let $e_2 = 0$, then $\dot{V}_1$ will be negative definite. Therefore, the Lyapunov function should be modified as: $V_2 = \frac{1}{2}(e_1^2 + e_2^2)$ to include the error variable $e_2$, then compute the time derivative for $e_2$ as:

$$\dot{e}_2 = \dot{x}_2 - \dot{\alpha}_1 = Ax_1x_4^2 - Ag\sin x_3 - \dot{\alpha}_1$$

$$= Ax_1x_4^2 - Ag\sin x_3 - c_1^2e_1 + c_1e_2 - \ddot{y}_{dx}. \tag{14}$$

By choosing the second stabilizing function $\alpha_2$, for $\sin x_3 = \alpha_2$, the sub-system $\dot{x}_2 = Ax_1x_4^2 - Ag\sin x_3$ can be stabilized. Assume $\sin x_3$ to be a virtual control, an error variable should be introduced as: $e_3 = \sin x_3 - \alpha_2$. By substituting $e_3$ into Eq. (14), $\dot{e}_2$ will become:

$$\dot{e}_2 = Ax_1x_4^2 - Ag(e_3 + \alpha_2) + c_1e_2 - c_1^2e_1 - \ddot{y}_{dx}.$$

In order to prove the system stability, compute the time derivative for $V_2$ as:

$$\dot{V}_2 = e_1\dot{e}_1 + e_2\dot{e}_2$$

$$= -c_1e_1^2 - Age_2e_3 + Ax_1x_4^2e_2$$

$$+ e_2(e_1 - Ag\alpha_2 + c_1e_2 - c_1^2e_1 - \ddot{y}_{dx}).$$

Let $e_1 - Ag\alpha_2 + c_1e_2 - c_1^2e_1 - \ddot{y}_{dx} = -c_2e_2$, and $c_2 > 0$, then the stabilizing function can be obtained as: $\alpha_2 = \frac{1}{Ag}(c_2e_2 + c_1e_2 - c_1^2e_1 + e_1 - \ddot{y}_{dx})$. Now $\dot{e}_2$ and $\dot{V}_2$ can be denoted as:

$$\dot{e}_2 = Ax_1x_4^2 - Age_3 - c_2e_2 - e_1,$$

$$\dot{V}_2 = -c_1e_1^2 - c_2e_2^2 - Age_2e_3 + Ax_1x_4^2e_2.$$

Therefore, $\dot{V}_2$ is indefinite.

Step 3: Similarly repeat the previous steps, the Lyapunov function $V_3$ is modified to involve error variable $e_3$. The time derivative of $e_3$ is computed as:

$$\dot{e}_3 = \dot{x}_3\cos x_3 - \dot{\alpha}_2$$

$$= x_4\cos x_3 - \frac{1}{Ag}[(c_1 + c_2)\dot{e}_2 + (1 - c_1^2)\dot{e}_1 - \ddot{y}_{dx}]$$

$$= x_4\cos x_3 - \frac{1}{Ag}[(c_1 + c_2)(-Age_3 - c_2e_2 - e_1)$$

$$+ (1 - c_1^2)(e_2 - c_1e_1) - \ddot{y}_{dx}] - \frac{1}{g}(c_1 + c_2)x_1x_4^2 \tag{15}$$

Choose the third stabilizing function $\alpha_3$ again, for $x_4\cos x_3 = \alpha_3$, the sub-system $\dot{x}_3 = x_4$ can be stabilized. Assume $x_4\cos x_3$ to be a virtual control, an error variable $e_4$ can be defined as: $e_4 = x_4\cos x_3 - \alpha_3$. Substituting $e_4$ into Eq. (15), and re-arranging $\dot{e}_3$ yield:

$$\dot{e}_3 = e_4 + \alpha_3 - \frac{1}{Ag}[(c_1 + c_2)(-Age_3 - c_2e_2 - e_1)$$

$$+ (1 - c_1^2)(e_2 - c_1e_1) - \ddot{y}_{dx}]$$

$$- \frac{1}{g}(c_1 + c_2)x_1x_4^2.$$

In order to prove the system stability, re-modify the Lyapunov function as: $V_3 = \frac{1}{2}(e_1^2 + e_2^2 + e_3^2)$, and take its time derivative:

$$\dot{V}_3 = e_1\dot{e}_1 + e_2\dot{e}_2 + e_3\dot{e}_3 = -c_1e_1^2 - c_2e_2^2 + e_3e_4$$

$$+ e_3\{-Age_2 + \alpha_3 - \frac{1}{Ag}[(c_1 + c_2)(-Age_3$$

$$- c_2e_2 - e_1) + (1 - c_1^2)(e_2 - c_1e_1) - \ddot{y}_{dx}]\}$$

$$+ Ax_1x_4^2e_2 - \frac{1}{g}(c_1 + c_2)x_1x_4^2e_3$$

Assume: $-Age_2 + \alpha_3 - \frac{1}{Ag}[(c_1 + c_2)(-Age_3 - c_2e_2 - e_1) + (1 - c_1^2)(e_2 - c_1e_1) - \ddot{y}_{dx}] = -c_3e_3$, and $c_3 > 0$, then get the stabilizing function $\alpha_3$ as:

$$\alpha_3 = -c_3e_3 + Age_2 + \frac{1}{Ag}[(c_1 + c_2)(-Age_3 - c_2e_2$$

$$- e_1) + (1 - c_1^2)(e_2 - c_1e_1) - \ddot{y}_{dx}].$$

After rearrangement of $\dot{e}_3$ and $\dot{V}_3$, they are described as:

$$\dot{e}_3 = -c_3e_3 + e_4 + Age_2 - \frac{1}{g}(c_1 + c_2)x_1x_4^2,$$

$$\dot{V}_3 = -c_1e_1^2 - c_2e_2^2 - c_3e_3^2 + e_3e_4 + Ax_1x_4^2e_2$$

$$- \frac{1}{g}(c_1 + c_2)x_1x_4^2e_3.$$

The result of $\dot{V}_3$ is indefinite conspicuously.

Step 4: The final step modifies the Lyapunov function $V_4$ to include the error variable $e_4$, then takes the time derivative operation for $V_4$ and $e_4$:

$$\dot{e}_4 = \dot{x}_4\cos x_3 - x_4\dot{x}_3\sin x_3 - \dot{\alpha}_3 = u_x'\cos x_3 - x_4^2\sin x_3 + c_3\dot{e}_3 - Ag\dot{e}_2 - \frac{1}{Ag}[(c_1 + c_2)(-Ag\dot{e}_3 - c_2\dot{e}_2 - \dot{e}_1) + (1 - c_1^2)(\dot{e}_2 - c_1\dot{e}_1) - y_{dx}^{(4)}].$$

By eliminating the differential terms, the above equation is rearranged into:

$$\dot{e}_4 = u_x'\cos x_3 - x_4^2\sin x_3 + (c_1 + c_2 + c_3)[-c_3e_3 + e_4 + Age_2 - \frac{1}{g}(c_1 + c_2)x_1x_4^2] - [Ag + \frac{1}{Ag}(1 - c_1^2 - c_1c_2 - c_2^2)](Ax_1x_4^2 - Age_3 - c_2e_2 - e_1) + \frac{1}{Ag}(2c_1 + c_2 - c_1^3)(-c_1e_1 + e_2) + \frac{1}{Ag}y_{dx}^{(4)} \quad (16)$$

In order to prove system stability, choose the Lyapunov function as:

$$V_4 = \frac{1}{2}(e_1^2 + e_2^2 + e_3^2 + e_4^2).$$

According to Eqs. (13) - (16), the time derivative of $V_4$ turns out to be:

$$\dot{V}_4 = -c_1e_1^2 - c_2e_2^2 - c_3e_3^2 + e_4\{u_x'\cos x_3 - x_4^2\sin x_3 + (c_1 + c_2 + c_3)e_4 + [A^2g^2 + 2 - (c_1^2 + c_2^2 + c_3^2 + c_1c_2 + c_2c_3 + c_1c_3)]e_3 + [Ag(c_1 + 2c_2 + c_3) + \frac{1}{Ag}(2c_2 - c_1^2c_2 - c_1c_2^2 - c_2^3 + 2c_1 - c_1^3)]e_2 + [Ag + \frac{1}{Ag}(1 - 3c_1^2 - 2c_1c_2 - c_2^2 + c_1^4)]e_1 + \frac{1}{Ag}y_{dx}^{(4)}\} + Ax_1x_4^2e_2 - \frac{1}{g}(c_1 + c_2)x_1x_4^2e_3 - [A^2g + \frac{1}{g}(1 + c_1c_2 + c_1c_3 + c_2c_3)]x_1x_4^2e_4$$

For calculation convenience, several parameters have to be pre-defined as:

$$\xi = \{u_x'\cos x_3 - x_4^2\sin x_3 + (c_1 + c_2 + c_3)e_4 + [A^2g^2 + 2 - (c_1^2 + c_2^2 + c_3^2 + c_1c_2 + c_2c_3 + c_1c_3)]e_3 + [Ag(c_1 + 2c_2 + c_3) + \frac{1}{Ag}(2c_1 + 2c_2 - c_1^2c_2 - c_1c_2^2 - c_2^3 - c_1^3)]e_2 + [Ag + \frac{1}{Ag}(1 - 3c_1^2 - 2c_1c_2 - c_2^2 + c_1^4)]e_1 + \frac{1}{Ag}y_{dx}^{(4)}\} \quad (17)$$

$B_1 = -\frac{1}{g}(c_1 + c_2)$, $B_2 = -[A^2g + \frac{1}{g}(1 + c_1c_2 + c_1c_3 + c_2c_3)]$, and $\lambda = x_1x_4^2$ Consequently, $\dot{V}_4$ can be denoted as:

$$\begin{aligned}\dot{V}_4 &= -c_1e_1^2 - c_2e_2^2 - c_3e_3^2 + \xi e_4 + A\lambda e_2 + B_1\lambda e_3 + B_2\lambda e_4 \\ &\le -c_1e_1^2 - \frac{c_2}{2}e_2^2 - \frac{c_3}{2}e_3^2 + \xi e_4 - \frac{c_2}{2}e_2^2 + A|\lambda||e_2| - \frac{c_3}{2}e_3^2 + |B_1||\lambda||e_3| + |B_2||\lambda||e_4| \\ &\le -c_1e_1^2 - \frac{c_2}{2}e_2^2 - \frac{c_3}{2}e_3^2 + \xi e_4 - \frac{c_2}{2}(|e_2| - \frac{1}{c_2}A|\lambda|)^2 + \frac{A^2\lambda^2}{2c_2} - \frac{c_3}{2}(|e_3| - \frac{1}{c_3}|B_1||\lambda|)^2 + \frac{1}{2c_3}B_1^2\lambda^2 - \frac{c_4}{2}(|e_4| - \frac{1}{c_4}|B_2||\lambda|)^2 + \frac{c_4}{2}e_4^2 + \frac{B_2^2\lambda^2}{2c_4} \\ &= -c_1e_1^2 - \frac{c_2}{2}e_2^2 - \frac{c_3}{2}e_3^2 - \frac{c_2}{2}(|e_2| - \frac{1}{c_2}A|\lambda|)^2 - \frac{c_3}{2}(|e_3| - \frac{1}{c_3}|B_1||\lambda|)^2 - \frac{c_4}{2}(|e_4| - \frac{|B_2|}{c_4}|\lambda|)^2 + e_4(\xi + \frac{c_4}{2}e_4) + \frac{1}{2}(\frac{A^2}{c_2} + \frac{B_1^2}{c_3} + \frac{B_2^2}{c_4})\lambda^2.\end{aligned}$$

Therefore $\dot{V}_4$ can be written as:

$$\dot{V}_4 \le -c_1e_1^2 - \frac{c_2}{2}e_2^2 - \frac{c_3}{2}e_3^2 + e_4(\xi + \frac{c_4}{2}e_4) + \frac{1}{2}(\frac{A^2}{c_2} + \frac{B_1^2}{c_3} + \frac{B_2^2}{c_4})\lambda^2.$$

Now, the $\dot{V}_4$ is ensured $\dot{V}_4 \le 0$, if $\dot{V}_4$ satisfies two conditions of:

(i) $\xi + \frac{c_4}{2}e_4 = -c_4e_4$, $c_4 > 0$, (18)

(ii) $c_m\|e_1, e_2, e_3, e_4\|^2 \ge \frac{1}{2}(\frac{A^2}{c_2} + \frac{B_1^2}{c_3} + \frac{B_2^2}{c_4})\lambda^2$, with $c_m \equiv \min\{c_1, \frac{c_2}{2}, \frac{c_3}{2}, c_4\}$, (19)

where $\|e_1, e_2, e_3, e_4\|^2 = e_1^2 + e_2^2 + e_3^2 + e_4^2$, $\|e_n\|$ is $L_2$ norm. Furthermore, the EM force from the MS actuators can be found by solving Eqs. (17) and (18) to get:

$$\xi = -\frac{3}{2}c_4e_4,$$

$$u_x' = \frac{1}{\cos x_3}\{x_4^2\sin x_3 - (c_1 + c_2 + c_3 + \frac{3}{2}c_4)e_4 - [A^2g^2 + 2 - (c_1^2 + c_2^2 + c_3^2 + c_1c_2 + c_2c_3 + c_1c_3)]e_3 - [Ag(c_1 + 2c_2 + c_3) + \frac{1}{Ag}(2c_1 + 2c_2 - c_1^2c_2 - c_1c_2^2 - c_2^3 - c_1^3)]e_2. - [Ag + \frac{1}{Ag}(1 - 3c_1^2 - 2c_1c_2 - c_2^2 + c_1^4)]e_1 - \frac{1}{Ag}y_{dx}^{(4)}\}$$

To solve Eq. (11), the EM force for X-axis sub-system is obtained as:

$$F_1a_1 + F_2a_2 = \frac{1}{\cos x_3}[(J_{px} + J_b + m_b x_1^2)u_x' + m_b g x_1 \cos x_3 + 2m_b x_1 x_2 x_4].$$

By the same procedures, the other EM force for the Y-axis is obtained as:

$$F_1b_1 + F_2b_2 = \frac{1}{\cos x_7}[(J_{py} + J_b + m_b x_5^2)u_y' + m_b g x_5 \cos x_7 + 2m_b x_5 x_6 x_8].$$

In a general case, for $F_1$ acting on the $P_1(a_1, b_1)$ and $F_2$ on the $P_2(a_2, b_2)$, the proposed system needs extra auxiliary equations or boundary conditions to solve the actuator force $F_1$ and $F_2$. By special arrangement for hardware configuration, $F_1$ acts at the point $P_1(a_1, 0)$ and $F_2$ acts at the point $P_2(0, b_2)$. Therefore, the EM force can be expressed as:

$$F_1 = \frac{1}{a_1 \cos x_3}[(J_{px} + J_b + m_b x_1^2)u_x' + m_b g x_1 \cos x_3 + 2m_b x_1 x_2 x_4],$$

$$F_2 = \frac{1}{b_2 \cos x_7}[(J_{py} + J_b + m_b x_5^2)u_y' + m_b g x_5 \cos x_7 + 2m_b x_5 x_6 x_8].$$

Finally, it can be concluded that, as long as $c_1$, $c_2$, $c_3$,$c_4$ are chosen to satisfy the condition of Eq. (19), $\dot{V}_4$ should be negative definite. To satisfy the condition of Eq. (19), only trials-and-error is adopted to tune the combination of $c_1$, $c_2$, $c_3$ and$c_4$ to reach an optimal system response. On the other hand, by using the Lasalle-Yoshizawa theory (Miroslav *et al*. 1995), one can be sure that under the condition $\cos x_3 \neq 0$, the system is stable. After derivations, this system is further simplified before software implementation, so that all parameters can be substituted and included into the program. The system equations for the X-axis are obtained as:

$$\begin{aligned}
\dot{x}_1 &= x_2 \\
\dot{x}_2 &= 0.7143 x_1 x_4^2 - 7.0073 \sin x_3 \\
\dot{x}_3 &= x_4 \\
\dot{x}_4 &= \frac{1}{0.010324 + 0.067 x_1^2}[(0.225F_1 - 0.6573x_1)\cos x_3 - 0.134 x_1 x_2 x_4],
\end{aligned} \tag{20}$$

$$\begin{aligned}
e_1 &= x_1 - y_{dx} \\
e_2 &= x_2 + c_1 e_1 - \dot{y}_{dx}
\end{aligned} \tag{21}$$

$$e_3 = \sin x_3 - 0.1427(c_2 e_2 + c_1 e_2 - c_1^2 e_1 + e_1 - \ddot{y}_{dx}) \tag{22}$$

$$e_4 = x_4 \cos x_3 + c_3 e_3 - 7.0073 e_2 - 0.1427[(c_1 + c_2)(-7.0073 e_3 - c_2 e_2 - e_1) + (1 - c_1^2)(e_2 - c_1 e_1) - \ddot{y}_{dx}] \tag{23}$$

$$u_x' = \frac{1}{\cos x_3}\{x_4^2 \sin x_3 - (c_1 + c_2 + c_3 + \frac{3}{2}c_4)e_4 - [49.1036 + 2 - (c_1^2 + c_2^2 + c_3^2 + c_1 c_2 + c_2 c_3 + c_1 c_3)]e_3 - [7.0073(c_1 + 2c_2 + c_3) + 0.1427(2c_1 + 2c_2 - c_1^2 c_2 - c_1 c_2^2 - c_2^3 - c_1^3)]e_2 - [7.0073 + 0.1427(1 - 3c_1^2 - 2c_1 c_2 - c_2^2 + c_1^4)]e_1 - 0.1427 y_{dx}^{(4)}\} \tag{24}$$

$$F_1 = \frac{1}{0.225 \times \cos x_3}[(0.010324 + 0.067 x_1^2)u_x' + 0.65727 x_1 \cos x_3 + 0.134 x_1 x_2 x_4]. \tag{25}$$

Similarly, the system equation for Y axis is:

$$\begin{aligned}
\dot{x}_5 &= x_6 \\
\dot{x}_6 &= 0.7143 x_5 x_8^2 - 7.0073 \sin x_7 \\
\dot{x}_7 &= x_8 \\
\dot{x}_8 &= \frac{1}{0.016774 + 0.067 x_5^2}[(0.185F_2 - 0.6573x_5) \cdot \cos x_7 - 0.134 x_5 x_6 x_8],
\end{aligned} \tag{26}$$

$$e_5 = x_5 - y_{dy},\ e_6 = x_6 + c_5 e_5 - \dot{y}_{dy}, \tag{27}$$

$$e_7 = \sin x_7 - 0.1427(c_6 e_6 + c_5 e_7 - c_5^2 e_5 + e_5 - \ddot{y}_{dy}) \tag{28}$$

$$e_8 = x_8 \cos x_7 + c_7 e_7 - 7.0073 e_6 - 0.1427[(c_5 + c_6)(-7.0073 e_7 - c_6 e_6 - e_5) + (1 - c_5^2)(e_6 - c_5 e_5) - \ddot{y}_{dy}] \tag{29}$$

$$u_y' = \frac{1}{\cos x_7}\{x_8^2 \sin x_7 - (c_5 + c_6 + c_7 + \frac{3}{2}c_8)e_8 - [49.1036 + 2 - (c_5^2 + c_6^2 + c_7^2 + c_5 c_6 + c_6 c_7 + c_5 c_7)]e_7 - [7.0073(c_5 + 2c_6 + c_7) + 0.1427(2c_5 + 2c_6 - c_5^2 c_6 - c_5 c_6^2 - c_6^3 - c_5^3)]e_6 - [7.0073 + 0.1427(1 - 3c_5^2 - 2c_5 c_6 - c_6^2 + c_5^4)]e_5 - 0.1427 y_{dy}^{(4)}\} \tag{30}$$

$$F_2 = \frac{1}{0.185 \times \cos x_7}[(0.016774 + 0.067x_5^2)u_y' + 0.65727x_5\cos x_7 + 0.134x_5x_6x_8]. \quad (31)$$

In these equations, $e_1 \sim e_4$ are the error variables, $c_1 \sim c_4$ are the controller parameters, and $y_{dx}$ is the tracking target for the X-axis; $e_5 \sim e_8$ are the error variables, $c_5 \sim c_8$ are the controller parameters, and $y_{dy}$ is the tracking target for the Y-axis; $F_1$ and $F_2$ are the controlled EM force for both MS actuators, respectively. According to Eqs. (20) ~ (31), the controller driving program can be formulated and organized. The parameters $c_1 \sim c_4$, and $c_5 \sim c_8$ are determined to satisfy the Lyapunov function for system stability. Eqs. (25) and (31) are manipulated to obtain the EM force for each MS actuator, and the EM coil current can be calculated from Eq. (1).

## VI. SYSTEM VERIFICATION

In the ball and plate system, the feedback data such as the ball position, ball velocity, plate deflection angle and plate deflection angle velocity are obtained from these two sub-systems as the state variables. The ball position and plate deflection angle thus obtained can be plotted for demonstration. In order to reduce measurement error, these quantified digital data are output directly from the CPU's serial port, and the software "Excel" is then employed to draw the output. The system performance is verified by two conditions: (a) random location stabilization, and (b) curve trajectory tracking. The sampling rate is 10 ms for all system tests.

In the proposed system, the plate is supported by the pivot at the center and two MS actuators, one on each side. According to the feedback state variables from sensors, the controller drives these two MS actuators to change plate deflection angles $\theta_x$ and $\theta_y$ to direct the ball to roll to a stable location. The ball begins rolling initially at any location, but will be controlled to roll to the predicted stable location on the plate. The control law determines which MS actuator should contribute how much effort to change the balance situation. The disturbance is randomly applied onto the ball to test the stiffness and stability of the system performance.

### 1. System Stability Test 1

In test 1, the system is initialized at: ($x$, $\dot{x}$, $\theta_x$, $\dot{\theta}_x$, $y$, $\dot{y}$, $\theta_y$, $\dot{\theta}_y$) = (0.14, 0, -0.04, 0, 0.11, 0, –0.04, 0), with control parameters ($c_1$, $c_2$, $c_3$, $c_4$, $c_5$, $c_6$, $c_7$, $c_8$) = (3.5, 6.5, 25, 10, 3.5, 6.5, 25, 10). In the proposed system, the ball position should be stabilized at the expected location on the plate regardless of the initial condition. In this test, the ball should be stabilized at the central point of the plate with robustness.

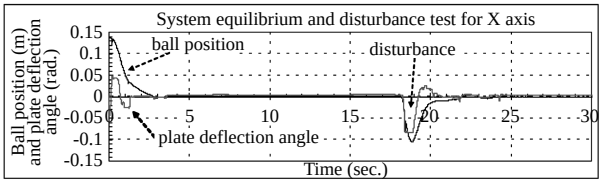


Fig. 7 System equilibrium and disturbance test for X axis

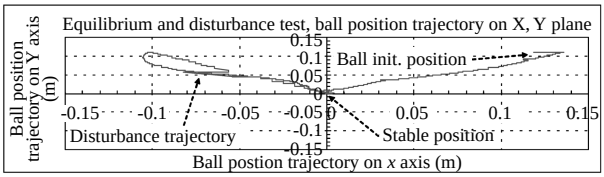


Fig. 8 System equilibrium and disturbance test, ball position on X-Y plane

After the control sequence starts, the ball and plate oscillates, but after three seconds, the ball is settled at the plate's central location, and the plate angle $\theta_x$ and $\theta_y$ are settled at 0 rad. In order to verify the robustness of the proposed system, the ball was pushed by hand toward the second quadrant as an input disturbance. The ball and plate system oscillated again and then settled after five seconds for the ball to return to the plate's central location again. Fig. 7 shows the relationship between ball position and plate deflection angle on the time domain. Similar results are demonstrated for the Y-axis. Fig. 8 shows the ball position trajectory on the X-Y plane. As can be seen, the controller drives the ball to roll the shortest path to approach the stable location.

### 2. System Oscillatory Test 2

To test the oscillatory tracking performance, the trajectory planning unit needs to predetermine the stable position

$$\text{Let, } n = \text{int}\left[\left(\sum_{i=0}^{k} T_i\right)/T_P\right], \quad (32)$$

where int[.] is an integer function, $T_i$ is the controller sampling interval, and $T_P$ is the stable position transfer period. The stable position function is predetermined as:

$$P(x, y) = A_m\cos\left(\frac{2n+1}{4}\pi\right)\hat{x} + B_m\sin\left(\frac{2n+1}{4}\pi\right)\hat{y} = y_{dx}\hat{x} + y_{dy}\hat{y}, \quad (33)$$

where $A_m$ and $B_m$ are the amplitudes, and $\hat{x}$ and $\hat{y}$ are unit vectors for the X- and Y-axis respectively. In

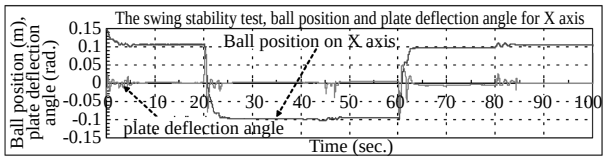


Fig. 9 Oscillatory stability test, ball position and plate deflection angle for X-axis

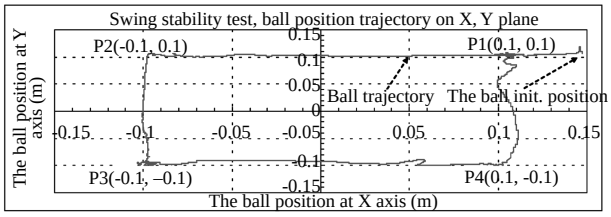


Fig. 10 Oscillatory stability and equilibrium test of ball position trajectory on the X-Y plane

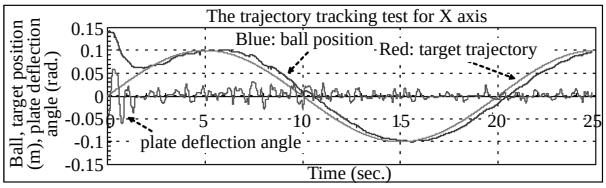


Fig. 11 Circular trajectory tracking on X-axis

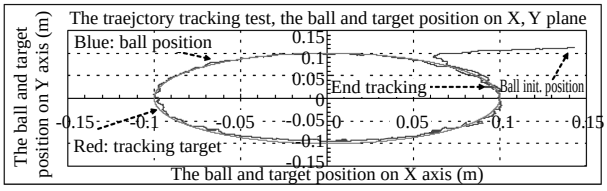


Fig. 12 Circular trajectory tracking on X-Y plane

this test, let $T_i$ = 0.02 seconds, $T_P$ = 20 seconds, and $A_m = B_m = 0.1 \times \sqrt{2}$ m. In each sampling, two additional calculations according to Eqs. (32) and (33) are needed for $n$ = 0, 1, 2, ···, $n$. The ball should be stabilized at the predetermined location: $P(x, y) = P1$ (0.1, 0.1) → $P2$ (–0.1, 0.1) →$P3$ (–0.1, –0.1) → $P4$ (0.1, –0.1) → $P1$ (0.1, 0.1) and so on, with each transfer cycle of 20 seconds. The system initial condition is set as: ($x$, $\dot{x}$, $\theta_x$, $\dot{\theta}_x$, $y$, $\dot{y}$, $\theta_y$, $\dot{\theta}_y$) = (0.14, 0, –0.05, 0, 0.12, 0, –0.04, 0), and control parameter ($c_1$, $c_2$, $c_3$, $c_4$, $c_5$, $c_6$, $c_7$, $c_8$) = (3.5, 7.5, 25, 13, 3, 6, 22, 10). Fig. 9 shows the relationship between ball position and plate deflection angle in the oscillatory performance for the X-axis, and likewise for the Y-axis. Fig. 10 plots the ball position trajectory on the X-Y plane for the oscillation test. The ball starts to roll from the initial location, then goes through four different stable points and is held for 20 seconds at each stable point.

### 3. Trajectory Tracking Test 3

This test aims to verify the system tracking capability. Assume the tracking target to be:

$$y_d = (A_m \sin nt)\hat{x} + (B_m \cos nt)\hat{y} = y_{dx}\hat{x} + y_{dy}\hat{y}. \quad (34)$$

In this test, let $A_m = B_m$ = 0.1 m, and $n = 0.1\pi$. Under these parameters, the ball is expected to track a circle with radius of 0.1 m, the period is predicted to be 20 seconds per tracking cycle. To compare the amplitude and phase shift, an additional standard trajectory target waveform is plotted according to Eq. (34) by software package "Microsoft Excel", and added to Fig. 11 and Fig. 12 to offer tracking reference waveforms for examining the controller performance. The system initial condition is ($x$, $\dot{x}$, $\theta_x$, $\dot{\theta}_x$, $y$, $\dot{y}$, $\theta_y$, $\dot{\theta}_y$) = (0.14, 0, –0.05, 0, 0.11, 0, –0.04, 0), and the controller parameters are tuned to ($c_1$, $c_2$, $c_3$, $c_4$, $c_5$, $c_6$, $c_7$, $c_8$) = (3.5, 9.5, 35, 20, 2.5, 6.5, 25, 11). Fig. 12 shows the ball tracking trajectory on the X-Y plane. Since the system is limited by the sampling rate and system response, a constant phase difference exists between the ball position and its tracking trajectory. Because of the initial condition, the error on the X-axis is larger than that on the Y-axis at the starting phase, but the ball approaches the target position quickly after two seconds with overall tracking errors of less than ±20 mm.

## VII. CONCLUSIONS

This paper presents a simple ball and plate system using magnetic suspension actuators to drive a ball moving on a touch control panel (TCP). In the proposed system, two independent systems of similar characteristics are introduced for X-axis and Y-axis operation. Based on Lyapunov stability theory, the backstepping controller can be designed in four steps to achieve a specific control law, and can properly be implemented to easily reach the control performance for different objectives. The system hardware was originally fabricated to demonstrate the proposed concept, and the control software algorithm was programmed following the step-by-step formulations to activate system performance in the laboratory. To test the static and dynamic performance of the proposed system, three different experiments are carried out to verify the proposed system stability in different scenarios of control performance. The experiment results verify that the proposed

system using a pair of magnetic suspension actuators is a correct and effective configuration for a ball and plate system design, control and reliable operation. The proposed ball and plate system is not only feasible for control practice, but also valuable for industrial applications.

## ACKNOWLEDGMENTS

This work is supported from National science Council under research project NSC93-2218-E006-016.

## REFERENCES

Andreev, F., Auckly D., Gosavi S., Kapitanski L., Kelkar A., White W., 2002, "Matching, Linear Systems, and the Ball and Beam," *Automatica*, Vol. 38, pp. 2147-2152.

Cygnal, *Cygnal Integrated Products Inc. for C8051F020 Data Sheet*, Available: www.silabs.com.

HUMUSOFT, *HUMUSOFT Real Time Toolbox for use with MATLAB Users Manual*, Abailable: www.humusoft.cz.

HUMUSOFT, *HUMUSOFT CE151 Ball & Plate Apparatus Users Manual*, Abailable: www.humusoft.cz.

Khalil, H. K., 2002, *Nonlinear Systems*, 3rd ed., Prentice Hall, Upper Saddle River, NJ, USA, pp. 589-603.

Knuplez A., Chowdhury A., Svecko R., 2003, "Modeling and Control Design for the Ball and Plate System," *2003 IEEE International Conference on Industrial Technology*, Vol. 2, pp. 1064-1067.

Lin, C. E., Jou, H. L., 1993, "Force Model Identification for Magnetic Suspension System via Magnetic Field Measurement," *IEEE Transactions on Instrumentation and Measurement.*, Vol. 42, pp. 767-771.

Lin, C. E., Ker, C. C., Wang, R. T., Chen, C. L., 2005, "A New Ball and Beam System Using Magnetic Suspension Actuator", *IEEE Industrial Electronics Conference*, Raleigh, NC. USA.

Pradel, G., Jin, Z. K., 1993, "An Insect-based Approach to Autonomous Mobile Robot Navigation," *1993. Proceedings of the IECON '93., International Conference on Industrial Electronics, Control, and Instrumentation*, Vol. 3, pp. 1448-1453.

Rad, A. B., Chan, P. T., Lo, W. L., and Mok, C. K., 2003, "An Online Learning Fuzzy Controller," *IEEE Trans. on Industrial Electronics*, Vol. 50, Issue 5, pp. 1016-1021.

Tsai, C.-H., Liu, J.-S., and Lin, W.-S., 1996, "A Neuro-Fuzzy Logic Controller for Trajectory Tracking of Uncertain Robots," *1996 IEEE International Conference on Robotics and Automation*, Vol. 2, pp. 1929-1934.

Tai, H. M., 1992, "Trajectory Tracking using Neural Networks", *ISCAS '92. Proceedings, 1992 IEEE International Symposium on Circuits and Systems*, Vol. 6, pp. 2929 - 2932.

Miroslav, K., Kanellakopoulos, I., Kokotović, P., 1995, *Nonlinear and Adaptive Control Design*, John Wiley & Sons, New York, USA, pp. 22-120.

Yubazaki, N., Jianqiang, Yi, Otani, M., Unemura, N., Hirota, K., 1997, "Trajectory Tracking Control of Unconstrained Objects Based on the SIRMs Dynamically Connected Fuzzy Inference Model, " *Proceedings of the Sixth IEEE International Conference on Fuzzy Systems*, Vol. 2, pp. 609-614.

Zhao, J., and Kanellakoulos, I., 1998, "Flexible Backstepping Design for Tracking and Disturbance Attenuation," *International Journal of Robust and Nonlinear Control*, Vol. 8, pp. 331 - 348.

***Manuscript Received: Mar. 29, 2006***
***Revision Received: Aug. 05, 2006***
***and Accepted: Sep. 10, 2006***